# Adsorption of Nitric Oxide in Aqueous Slurries of Activated Carbon: Transport Rates by Moment Analysis of Dynamic Data

**HIROO NIIYAMA**
**and**
**J. M. SMITH**
**University of California**
**Davis, California 95616**

Moment analysis of input-response data for three-phase slurry reactors is shown to be useful for determining mass transport rate coefficients. Data for the nitric oxide-water activated carbon system indicated that bubble-to-liquid transport, intraparticle diffusion, and the adsorption step could all influence the adsorption rate for high concentrations of carbon particles.

## SCOPE

Three-phase slurry reactors combine multiple mass transfer steps with surface (of the solid particles) processes of adsorption and reaction. Attempts to evaluate the rates of the significant transport and surface steps have been limited to reaction studies (for example, Sherwood and Farkas, 1966; Komiyama and Smith, 1975) where steady state, or pseudo steady state, conditions were obtained. The objectives in our work were to develop and apply a method for evaluating transport and surface rate coefficients from dynamic adsorption experiments on a three-phase system in which the gas is bubbled through an agitated slurry.

Misic and Smith (1971) considered the special case in which there was no retardation of the rate due to intraparticle diffusion and for which the adsorption step at the particle surface occurred at equilibrium concentrations. In this situation, for linear processes, it was possible to derive explicit equations for the concentration in the effluent gas bubbles as a function of time. Such equations could then be compared with measured breakthrough curves. Moment analysis of response curves of concentration in the liquid phase of a two-phase slurry has been used to evaluate liquid-to-solid mass transport (Furusawa and Smith, 1973*b*; Furusawa and Suzuki, 1975), but these treatments did not include gas bubble-to-liquid mass transfer.

For a three-phase system in which all the transport and surface adsorption steps are considered, solution of the mass conservation differential equations for the concentration as a function of time gives results, even for linear processes, which are too complex to analyze. However, the equations for the moments of the response curves-to-pulse inputs are relatively simple. These simple equations can be then compared with moments of experimental response curves to determine rate coefficients.

The method is illustrated with breakthrough curves measured for the adsorption of nitric oxide in aqueous slurries of activated carbon particles at 25°C and 1 atm. We were particularly interested in evaluating the effect of intraparticle diffusion and in determining the rate constant $k_{ads}$ for adsorption on the active sites of the carbon particles. To our knowledge, there is no published information on adsorption rate constants for the nitric oxide-water-carbon system and little quantitative data for this constant for other slurry systems.

## CONCLUSIONS AND SIGNIFICANCE

Equations were derived for the first and second moments of the response in the gas phase to a pulse input of concentration for a three-phase slurry adsorber. The derivation includes all the mass transport processes from gas bubble to solid but is limited to first-order processes. The first absolute moment is a function of system's adsorption capacity, which was expressed in terms of the equilibrium constant for adsorption on the solid phase and the Henry's law constant for solubility in the liquid phase. The expression for the second moment is a summation of separate contributions for each of the mass transfer steps, the adsorption process, and for dispersion in the volumes (dead volumes) of the apparatus between sample injection and slurry and between slurry and concentration detector.

Step function inputs were found to be preferable experimentally to pulse inputs for our measurements. This is due primarily to the increased accuracy in calculating the second moment from the response (breakthrough curve) to a step function input. Equations are given for calculating moments from measured breakthrough curves.

Hiroo Niiyama is on leave from Tokyo Institute of Technology, Japan.

Analysis of the first moment data for the nitric-oxide-water-activated carbon slurry gave a value for Henry's law constant for nitric oxide in water in good agreement with the information in the literature. The adsorption isotherm for nitric oxide (from aqueous solution) on activated carbon was found to be linear up to a liquid concentration of $0.4 \times 10^{-6}$ mole/cm$^3$, which corresponds to an equilibrium gas concentration of about 20% at 1 atm pressure. The adsorption capacity of carbon for nitric oxide was low and gave an adsorption equilibrium constant of about 6.9 cm$^3$/g.

In an apparatus for slurries in which gas concentrations are measured, some free space above the liquid level is necessary to allow for disengagement and collection of gas bubbles. This volume and other dead volumes in the system provide for retention time and regions for dispersion. Even when such volumes are minimized, their effects can be important, particularly if the time required to saturate the liquid and adsorbent particles is low. The dead volumes, flow rates, and saturation times in our experiments with nitric oxide were such that corrections for dead volume effects were significant. Accurate values of such corrections to the moments can readily be obtained experimentally because such effects constitute additive terms to the moment equations. Since nitrogen is nearly insoluble in saturated sodium chloride solution, measured moments for this chemical system in the same apparatus were used to obtain dead-volume corrections.

Analysis of the second moment data for different flow rates and carbon particle sizes yielded values of rate coefficients for bubble-to-liquid mass transfer, intraparticle diffusivity, and adsorption at a site on the interior pore surface. Since we were primarily interested in the latter two coefficients, a sufficient concentration of carbon particles was used to decrease to a negligible magnitude the contribution of water-to-particle surface mass transfer. For the nitric oxide-water-carbon slurry, the rate for the smallest particle ($R = 0.0015$ cm) was determined by the bubble-to-liquid mass transport and the surface adsorption processes. For the larger particles ($R = 0.04$ to 0.083 cm), intraparticle diffusion also retarded the rate. The intraparticle diffusivity and adsorption rate constant were $1.8 \times 10^{-5}$ cm$^2$/s and $5.8 \times 10^{-2}$ cm$^3$/(g)(s), respectively. These results should be useful for development of processes for removal of nitric oxide from gases by adsorption and oxidation (with air) in aqueous slurries of activated carbon.

The extent of mixing of the gas bubbles in a slurry can, in general, affect performance. However, it was shown that for either very rapid or very slow mass transfer from bubble to liquid, for example, for very soluble or for slightly soluble gases, that the mixing state of the bubbles does not affect the analysis of the data. The nitric oxide-water system corresponds to the slightly soluble extreme. For intermediate cases, a test was proposed to indicate whether the bubble mixing condition influences the behavior of the system.

---

Mass transfer of adsorbate in a three-phase slurry reactor will be treated as a series process consisting of the following steps:

1. Transport within the gas bubble to the bubble-liquid interface.
2. Bubble interface-to-bulk liquid transfer (according to a transfer coefficient $k_L$).
3. Bulk liquid-to-adsorbent particle transport ($k_s$).
4. Intraparticle diffusion ($D_e$).
5. Adsorption on the interior pore surface ($k_{ads}$).

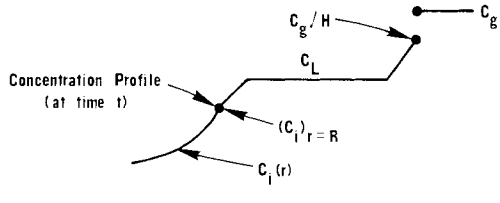


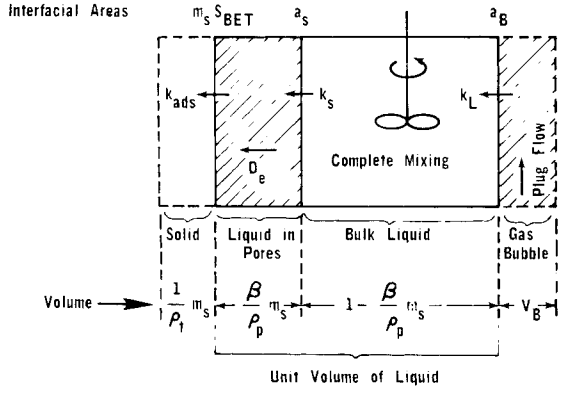


Fig. 1. Schematic diagram of mass transfer and adsorption in slurries.

This model requires that the resistance to transport in the bulk liquid is negligible, an assumption that is valid when the slurry is well agitated, as in our experiments. Since nitric oxide is but slightly soluble in water, a rate coefficient for step 1 is not required; the liquid-phase concentration at the bubble-liquid interface will be very close to the value corresponding to equilibrium with the bulk gas, that is, to $C_g/H$. The concentration profile corresponding to this model is shown in the upper part of Figure 1. The extensive properties, such as interfacial areas, volumes, and mass, of the reactor system, will be based upon a unit volume of liquid in the slurry, including the liquid that fills the pores of the adsorbent particles. The lower part of Figure 1 gives the areas and volumes on this basis and also indicates schematically the mass transport model.

The experimental data consisted of breakthrough curves measured for the effluent gas stream from the adsorber. From these data values for the moments could be calculated and compared with theoretical expressions. From such comparisons values of several of the rate coefficients could be obtained. The advantage of this approach is that it is relatively easy to derive explicit equations for the moments in terms of the rate coefficients when all the steps in the whole process are linear.

## THEORY

In a three-phase slurry system in which the gas is introduced as discrete bubbles through a disperser and the slurry is agitated, mixing in the bulk liquid is excellent so that the concentrations of adsorbate (nitric oxide) and adsorbent particles will be assumed to be uniform throughout the reactor. At this point it also will be supposed that the bubbles travel in upward plug flow; that is, there is no back mixing of bubbles. These assumptions

are customary (Siems and Weiss, 1957; Juvekar and Sharma, 1973; Misic and Smith, 1971; Komiyama and Smith, 1975), although plug flow for the gas bubbles may be questionable when the agitation is vigorous (Satterfield, 1970). It is shown later that this assumption is a valid one for our experimental conditions. It will also be assumed that the bubble size does not change as the bubble travels through the slurry and that the adsorption rate is first order. These conditions are closely met experimentally when the adsorbate is slightly soluble in the liquid or when its concentration in the gas is low.

#### Moment Equations for the Slurry ($z = 0$ to $L_1$)

For the described conditions, mass conservation equations for the adsorbate in the gas bubbles, in the liquid, and in the pores of the adsorbent particles are

$$-v_B V_B \frac{\partial C_g}{\partial z} - k_L a_B \left( \frac{C_g}{H} - C_L \right) = V_B \frac{\partial C_g}{\partial t} \quad (1)$$

$$\frac{1}{L_1} \int_0^{L_1} k_L a_B \left( \frac{C_g}{H} - C_L \right) dz - k_s a_s [C_L - (C_i)_{r=R}] = \left( 1 - m_s \frac{\beta}{\rho_p} \right) \frac{dC_L}{dt} \quad (2)$$

$$D_e \left( \frac{\partial^2 C_i}{\partial r^2} + \frac{2}{r} \frac{\partial C_i}{\partial r} \right) = \beta \frac{\partial C_i}{\partial t} + \rho_p \frac{\partial n}{\partial t} \quad (3)$$

where $C_g$, $C_L$, $C_i$, and $n$ are concentrations in the gas, bulk liquid, liquid in pores, and adsorbed on the pore surface. For reversible adsorption, the first-order rate equation is

$$k_{ads} \left( C_i - \frac{n}{K} \right) = \frac{\partial n}{\partial t} \quad (4)$$

If we imagine a pulse input of adsorbate into the gas stream entering the reactor, the initial and boundary conditions are

$$C_g = C_{go} \delta(0) \quad \text{at} \quad z = 0 \quad (5)$$

$$C_L = C_i = n = 0 \quad \text{at} \quad t = 0 \quad \text{for} \quad z \geq 0 \quad (6)$$

$$\left( \frac{\partial C_i}{\partial r} \right)_{r=0} = 0 \quad (7)$$

$$k_s a_s [C_L - (C_i)_{r=R}] - a_s D_e \left( \frac{\partial C_i}{\partial r} \right)_{r=R} = 0 \quad (8)$$

where $\delta(0)$ is the Dirac delta function which has an infinite value at $t = 0$. Equations (1) to (4) relate the gas concentration $C_g(z, t)$ to the rate coefficients $k_L$, $k_s$, $D_e$, $k_{ads}$. Misic and Smith (1971) considered a special case of the problem wherein intraparticle diffusion and adsorption rate were very fast, and they obtained a solution for $C_g(z, t)$ as a function of $k_L$ and $k_s$. For the more general case considered here, solution for $C_g(z, t)$ is not very helpful because the results are too complex to use for interpreting experimental data. However, the equations for the moments of the response curves are practical for evaluating rate constants. The moment expressions can be obtained from the solution $\tilde{C}_g(L_1, s)$ of Equations (1) to (8) in the Laplace domain, by using the expression

$$m_n = (-1)^n \lim_{s \to 0} \frac{d^n \tilde{C}_g(L_1, s)}{ds^n} \quad (9)$$

where $m_n$ is defined as

$$m_n = \int_0^\infty t^n C_g dt \quad (10)$$

and the first absolute and second central moments are

$$\mu'_{1,L_1} = \frac{m_1}{m_o} \quad (11)$$

$$\mu_{2,L_1} = \frac{1}{m_o} \int_0^\infty (t - \mu'_{1,L_1})^2 C_g dt = \frac{m_2}{m_o} - \left( \frac{m_1}{m_o} \right)^2 \quad (12)$$

The resulting expressions for the moments are

$$m_o = C_{go} \quad (13)$$

$$\mu'_{1,L_1} = \frac{m_s K + 1}{H} \left( \frac{V_L}{Q} \right) \quad (14)$$

$$\mu_{2,L_1} = \frac{2}{H} \left[ \left( \frac{1}{5} \frac{R}{D_e a_s} + \frac{1}{k_s a_s} \right) \left( m_s \frac{\beta}{\rho_p} + m_s K \right)^2 + \frac{m_s K^2}{k_{ads}} \right] \frac{V_L}{Q} + \left( \frac{m_s K + 1}{H} \right)^2 \frac{1 + e^{-\alpha L}}{1 - e^{-\alpha L}} \left( \frac{V_L}{Q} \right)^2 \quad (15)$$

where

$$\alpha = \frac{k_L a_B}{v_B V_B H} \quad (16)$$

These results were obtained by neglecting the term $V_B(\partial C_g/\partial t)$ in Equation (1). This term is small because the residence time of the gas bubble in the slurry is small, about 0.5 s in our experiments. It can be shown that the error in the moment equations due to this assumption is dependent upon the relative values of $V_B$ and $(m_s K + 1)/H$. For the experimental conditions used here, $V_B$ was but 2 to 5% of $(m_s K + 1)/H$.

#### Corrections for Dead Volume Effects

Before Equations (14) and (15) can be compared with moments of the experimentally measured response curves, corrections must be applied for the retention time and dispersion in the dead volumes. These volumes are the volume between injection point and the entrance of gas bubbles into the liquid (at $z = 0$) and the volume between the liquid level in the slurry ($z = L_1$) and the concentration detector. Such corrections are particularly important for a slurry system because it is necessary to have a bubble collecting space above the slurry liquid. This latter space is designated as the region $z = L_1$ to $z = L_2$ (see Figure 2).

If the retention times and dispersion effects in the dead volume can be described by linear processes, the

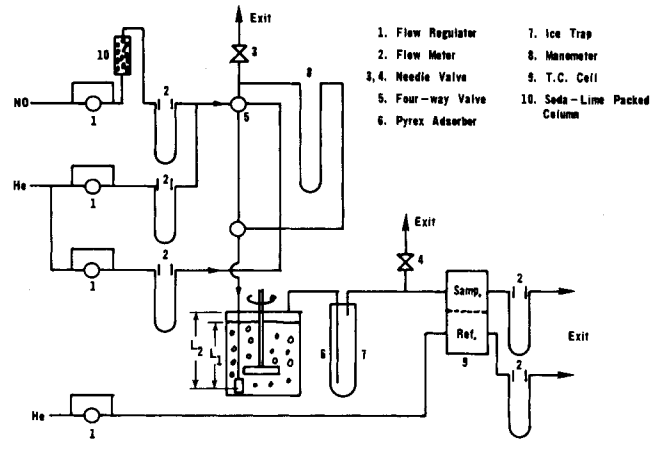


Fig. 2. Schematic diagram of apparatus.

moments at the detector, designated by subscript $D$, are those given by Equations (14) and (15) plus a term for the dead-volume contributions; that is

$$\mu'_{1,D} = \mu'_{1,L_1} + \mu'_{1,\text{d.v.}} \tag{17}$$

$$\mu_{2,D} = \mu_{2L,1} + \mu_{2,\text{d.v.}} \tag{18}$$

Rather than theoretically estimate expressions for the dead-volume contributions, our approach was to obtain $\mu'_{1,\text{d.v.}}$ and $\mu_{2,\text{d.v.}}$ from experimental breakthrough curves for a nearly insoluble system, nitrogen gas bubbling through a saturated sodium chloride solution. Then, $\mu'_{1,L_1}$ and $\mu_{2,L_1}$ could be calculated from Equations (17) and (18) and the measured values at the detector.

#### Moment Expressions for Breakthrough Curves

Second moments determined from responses to step-function inputs are probably more accurate than those from pulse inputs at our conditions. This is because one avoids the emphasis, given by the $t^2$ term in Equation (12), to the uncertain tail of the response curve. Hence, only breakthrough curves were measured. The relation between the solutions for $\tilde{C}_g$ in the Laplace domain for pulse input ($\delta$) and step input ($b$) is

$$\tilde{C}_g(z, s)_\delta = s\tilde{C}_g(z, s)_b \tag{19}$$

By using Equation (19) and the properties of the Laplace transformation, the moment equations in terms of the breakthrough curves are

$$\mu'_{1,D} = \frac{1}{(C_{g_o})_b}\int_0^\infty (C_{g_o} - C_g)_b\, dt \tag{20}$$

$$\mu_{2,D} = \frac{2}{(C_{g_o})_b}\int_0^\infty (C_{g_o} - C_g)_b\, t\, dt - (\mu'_{1,D})^2 \tag{21}$$

Equations (20) and (21) were employed with the experimental breakthrough curves $[C_g(t)]_b$ to obtain values for the moments for use in Equations (17) and (18).

#### Experimental

The slurry reactor was a cylindrical Pyrex vessel, about 13 cm high and 10 cm in diameter, equipped with an impeller and eight fixed baffles. The dimensions and geometry were the same as used and described by Furusawa and Smith (1973*a*). With this geometry, the energy dissipation rate (due to agitation) is known so that $k_L$ can be estimated from available correlations and compared with the result obtained by analyzing the experimental moment values. The gas stream (nitric oxide plus helium for adsorption runs, helium for purge or desorption runs, and nitrogen for dead-volume correction runs) was introduced through a fritted glass disk 1.2 cm in diameter, 2.1 cm in height, and located at the bottom of the reactor. The average height of the emerging gas bubbles was about 1.4 cm above the bottom of the vessel. The height of the slurry above this location was about 12.0 cm. The reactor and auxiliary apparatus are shown in Figure 2.

BPL activated carbon, whose properties are given in Table 1, were used as adsorbent. Prior to use, the particles were washed with distilled water and dried at 110°C to constant weight. Also, the large particles were boiled in distilled water to ensure that the pores were filled with liquid.

The nitric oxide (Liquid Carbonic Co.) contained small amounts of nitrogen dioxide and nitrogen, as determined by chromatographic analysis. Nitrogen dioxide was removed in a packed bed of soda lime (Figure 2). Since nitrogen was not adsorbed, the small amount (less than 3%) in the nitric oxide was not removed. The helium used had a stated purity of 99.99% and was not further purified. For the rate studies, the gas stream had a composition of 10% nitric oxide and 90% helium.

Table 1. Operating Conditions

A. Properties of Pittsburgh activated carbon, type BPL*

| | |
|---|---|
| Surface area, $S_{BET}$ | 1 050 ~ 1 150 m²/g |
| Solid-phase density, $\rho_t$ | 2.1 g/cm³ |
| Particle density, $\rho_p$ | 0.85 g/cm³ |
| Porosity, $\beta$ | 0.60 |
| Average initial particle radius,† $R$ | 0.0015, 0.040, 0.075, 0.12 cm |
| Mean pore radius in particles | 13Å |

B. Volumes of slurry, liquid, and solid particles
- Slurry: water = 1 015 cm³ and carbon = 200 g; equivalent to about 1 100 cm³ of slurry; $m_s$ = 0.197 g/cm³
- Water (for the measurements of $H$ and $k_L$) = 1 100 cm³

C. Concentration of inlet gas (NO in He)
- For equilibrium measurements: 2.5 to 20% NO
- For rate measurements: 10% NO

D. Other operating conditions
1. Gas flow rate = 3.33 to 10 cm³/s (at 25°C, 1 atm)
2. Impeller speed: 670 ± 40 rev/min
3. Temperature: 25 ± 2°C
   Pressure: 1 atm

* From data sheet, type BPL activated carbon, Calgon Corp., Pittsburgh, Pa. 15230, Mar. 1, 1972.

† Arithmetic average of sieve openings after particles have been pretreated in water to eliminate corners and edges. Pretreated shape is assumed to be spherical.

Table 1 also shows the range of gas flow rates and volumes of slurry, as well as other operating conditions.

#### Operating Procedure

Before each run, the slurry in place was pretreated with pure helium flow for at least 14 hr. The step function of nitric oxide plus helium gas was introduced by turning a four-way valve (5 in Figure 2). Pressure surges were minimized by adjusting the mercury columns in manometer [8] to the same level with needle valve [3]. This procedure gave a sharp change in concentration without fluctuations in flow rate. The gas flow from the reactor [6] passed through an ice trap [7] to eliminate water and then was divided into two streams. One stream at a constant rate of 0.83 cm³/s flowed through the thermal conductivity detector, and the other stream was vented to the hood. The volume of tubing, ice trap, and gas space above the slurry level in the reactor was minimized and amounted to about 250 cm³.

In order to reduce random experimental error, many runs were made at each set of operating conditions. Helium flowed through the reactor between runs for at least 20 mins after zero nitric oxide concentration was achieved, as noted by return of the detector signal to its original base line position. This required a total helium flow time of 30 to 90 min.

## EQUILIBRIUM RESULTS

Figure 3 is an example of the breakthrough curve data. The lower curve is for nitric oxide adsorption in the slurry, while the upper curve applies for $N_2$ in the same total volume (1 100 cm³) of a saturated aqueous sodium chloride solution. Nitrogen has a very low solubility in salt solutions, so that the breakthrough curve for this latter system provides an accurate measure of the moments $\mu'_{1,\text{d.v.}}$ and $\mu_{2,\text{d.v.}}$ in the dead-volume regions.

Curves such as those shown in Figure 3 were used to evaluate the solubility of nitric oxide in water and its adsorption equilibrium constant in the aqueous solution-activated carbon system. The method of calculation can be explained by reference to the areas marked I, II, III on the schematic breakthrough curve shown in Figure 4.

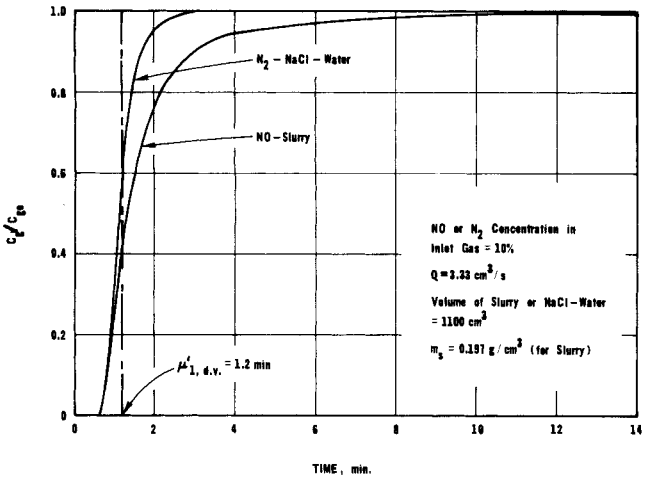


Fig. 3. Typical response curves for nitric oxide-slurry and nitrogen-sodium chloride-water systems.

Suppose, first, that the curve is for a gas which is insoluble in the liquid and that the concentrations correspond to those measured at the detector in the apparatus shown in Figure 2. If there were no dispersion in the dead volumes, the curve would rise vertically at a time equal to $\mu'_{1,d.v.}$. Owing to dispersion in the dead volumes, the actual breakthrough curve has the nonvertical shape shown in Figure 4. Equation (20) indicates that $\mu'_{1,d.v.}$ is equal to areas I + II. Alternately, $\mu'_{1,d.v.}$ can be found by locating a vertical line such that areas II and III are equal. If, now, the solubility of the gas is considered, $\mu'_{1,d.v.}$ would be determined by locating the vertical line such that area II is equal to area III plus the area corresponding to the amount of gas dissolved in the liquid. Figure 4 has been drawn to illustrate this case. Linke (1965) gives solubilities of oxygen and nitrogen in water at 25°C ($H_{O_2} = 32.3$, $H_{N_2} = 63.8$) and of nitrogen for a saturated sodium chloride solution ($H = 384$). The solid circle points in Figure 5 show the results of calculating $\mu'_{1,d.v.}$ by this method from the breakthrough curves for the nitrogen-salt solution system. For verification, breakthrough curves for oxygen-water and nitrogen-water were also measured at $Q = 3.33$ cm³/s. The resulting values of $\mu'_{1,d.v.}$ shown in Figure 5 indicate that the method for accounting for retention times in the dead volumes is dependable.

Figure 5 shows also values of $\mu'_{1,D}$ for the nitric oxide-slurry system at various flow rates calculated from breakthrough curve data by using Equation (20). According to Equations (17), the difference between $\mu'_{1,D}$ and $\mu'_{1,d.v.}$ gives $\mu'_{1,L_1}$, and by Equation (14) the slope of this line is equal to $(m_s K + 1)/H$. In order to determine $K$, the solubility $H$ must be established. While Linke (1965) gives 21.5 at 25°C for $H_{NO}$ in water, a curve of $\mu'_{1,D}$ vs. $V_L/Q$ for water without carbon particles and the $\mu'_{1,d.v.}$ line in Figure 5 can be used to calculate $H_{NO}$. Equation (14) with $m_s = 0$ is applicable. Analyzed in this way, our data give $H_{NO} = 22.5$, which agrees reasonably well with the literature value.

By using $H_{NO} = 22.5$ and the curve for $\mu'_{1,L_1}$ in Figure 5, $K$, which is equal to $(n/C_L)_{equil}$, is 6.86 cm³/g. These results are based upon data for a gas concentration of 10% nitric oxide in helium. Data points for all gas concentrations plotted as $C_L$ vs. $C_g$ and $n$ vs. $C_L$ are shown in Figure 6. The points for gas concentrations other than 10% nitric oxide were obtained from measurements at a single flow rate of 3.33 cm³/s for both adsorption and desorption.

The key feature of Figure 6 for our work is that the $n$ vs. $C_L$ and $C_g$ vs. $C_L$ isotherms are linear, since this assumption was employed in deriving Equations (14) and (15).

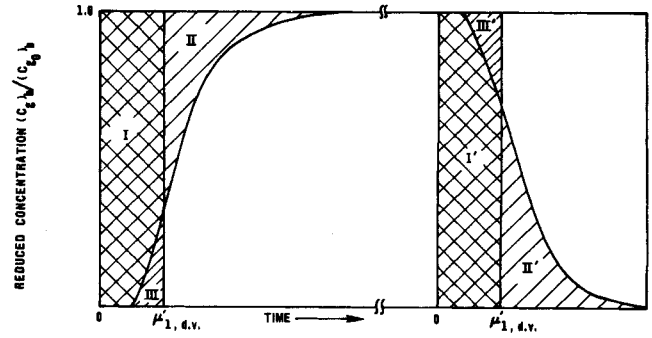


Fig. 4. Graphical integration method for isotherm determination.

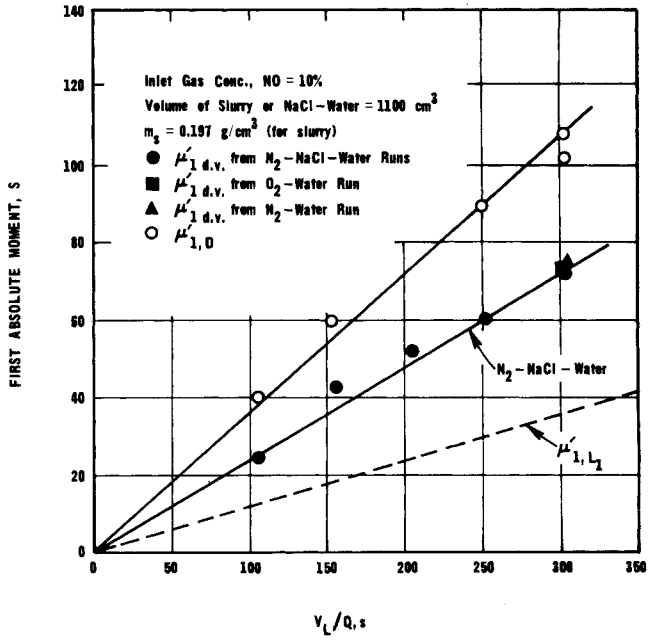


Fig. 5. First moment data.

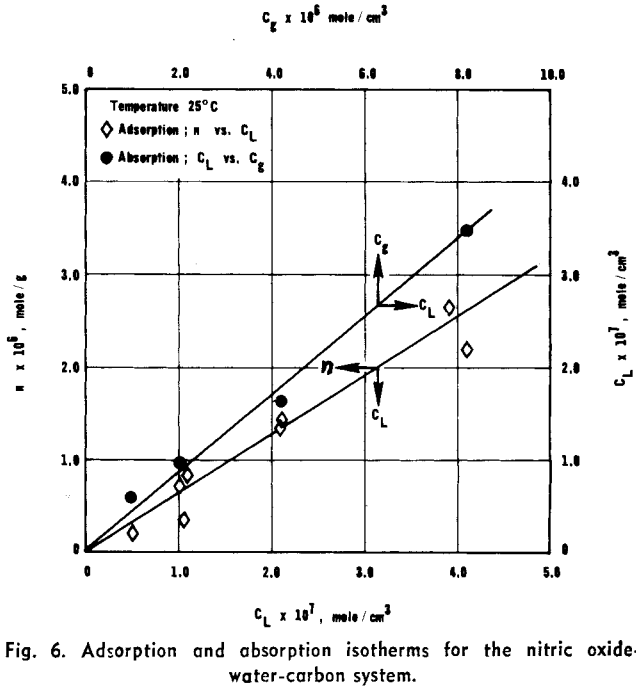


Fig. 6. Adsorption and absorption isotherms for the nitric oxide-water-carbon system.

Table 2. Bubble Properties

| $Q$, cm³/s | $v_B$, cm/s | $R_B$, cm | $V_B$*, † | $a_B$*, **, cm⁻¹ | $\mu_{2,d.v.}$, s² | $k_La_B$,†† s⁻¹ |
|---|---|---|---|---|---|---|
| 3.33 | 22.5 | 0.065 | $1.64 \times 10^{-3}$ | 0.075 | $15.0 \times 10^2$ | 0.019 |
| 4.00 | 22.5 | 0.065 | $1.94 \times 10^{-3}$ | 0.090 | $8.60 \times 10^2$ | 0.023 |
| 5.00 | 22.5 | 0.065 | $2.43 \times 10^{-3}$ | 0.112 | $7.60 \times 10^2$ | 0.028 |
| 6.67 | 22.5 | 0.065 | $3.23 \times 10^{-3}$ | 0.150 | $3.67 \times 10^2$ | 0.037 |
| 10.0 | 22.5 | 0.065 | $4.85 \times 10^{-3}$ | 0.224 | $1.62 \times 10^2$ | |

* Since our equations are based on unit volume of bubble and solid free liquid, the values of $V_B$ and $a_B$ listed here for water runs are different from those for slurry runs. A multiplication factor of 1.083 $\left( = \frac{1\,100}{1\,015} \right)$ should be used to obtain $V_B$ and $a_B$ for the slurry runs.

† Calculated from Equation (23).
** Calculated from Equation (22).
†† For nitric-oxide water runs (from data of Figure 8).

The correction term $\mu'_{1,d.v.}$ can also be obtained by estimating the dead volumes from the geometry of the apparatus between four-way valve [5, Figure 2] and the detector [9]. This method is less accurate and gave values of $\mu'_{1,d.v.}$ about 8% less than those obtained by response measurements with oxygen and nitrogen.

The equilibrium properties $H$ and $K$ could also be estimated from desorption runs, whose breakthrough curves are of the form shown on the right side of Figure 4. Thus, area II'-(area III') is the amount dissolved in the water and adsorbed on carbon particles, if a slurry is used. Such desorption curves returned to the baseline rather sharply, showing that the adsorption process was reversible. Values of $H$ and $K$ so obtained were in some cases larger and in some instances less than those obtained from the adsorption data. The points in Figure 6 are averages of adsorption and desorption results.

## BUBBLE PROPERTIES

The bubble-liquid interfacial area $a_B$ is required in order to evaluate the mass transfer coefficient $k_L$, although such separation of the product $k_L\, a_B$ is not necessary for determining the other rate coefficients. While we are chiefly interested in $D_e$ and $k_{ads}$ for the nitric oxide-slurry system, sufficient properties of the gas bubbles were established in order to determine, at least approximately, values for $k_L$.

If the bubbles are spherical, the area $a_B$ is related to bubble velocity $v_B$ and radius $R_B$ by

$$a_B = \left(\frac{Q}{V_L}\right)\frac{3}{R_B}\left(\frac{L}{v_B}\right) \qquad (22)$$

which is based upon $v_B$ being equal to the vertical component of the bubble velocity. All quantities in Equation (22) are known except $v_B$ and $R_B$. The velocity can be estimated from the total volume ($V_B$ $V_L$) of bubbles in the slurry by using the relation

$$v_B = \frac{QL}{(V_B V_L)} \qquad (23)$$

($V_B V_L$) was determined by measuring the increase in level of the liquid when gas was introduced through the disperser disk. The average velocity calculated from Equation (23) for measurements at several flow rates was 21.6 ± 4 cm/s when water was used in a narrow vertical tube without mechanical agitation. For slurries of carbon particles, the velocity was 19.7 ± 3 cm/s, measured in the same tube. A direct and probably more accurate method employed by Valentin (1967) gave 22.5 cm/s. Since the rise in liquid level was relatively small and the level was disturbed by bursting gas bubbles, $v_B$ = 22.5 cm/s was used in subsequent calculations.

The average bubble size was determined from high-speed (exposure time = 0.001 s) photographs of bubbles from the same disperser rising through water. The procedure was identical to that employed by Misic and Smith (1971). Visual measurements for 180 bubbles on projections of the photographs showed a radius range of 0.03 to 0.13 cm and a mean value of $R_B$ = 0.065 cm. Data for different gas flow rates showed no discernible change in $R_B$.

The interfacial areas calculated from these data and other bubble properties are shown in Table 2.

## DEAD-VOLUME DISPERSION ($\mu_{2,d.v.}$)

If Equation (15) is applied for liquid only ($m_s = 0$) and combined with Equation (18), the resulting expression for the moment at the detector is

$$\mu_{2,D} = \mu_{2,d.v.} + \left(\frac{1}{H^2}\right)\frac{1 + e^{-\alpha L}}{1 + e^{-\alpha L}}\left(\frac{V_L}{Q}\right)^2 \qquad (24)$$

For the nitrogen saturated sodium chloride solution, $H$ is large and $\alpha$ small. Hence the second term on the right side of Equation (24) can be evaluated with little error by expanding the exponential functions in a power series and by neglecting second degree and higher terms. The result is

$$\mu_{2,D} = \mu_{2,d.v.} + \frac{2}{H^2 \alpha L}\left(\frac{V_L}{Q}\right)^2 \qquad (25)$$

Using Equation (16) for $\alpha$ and Equation (23) for $Q/V_L$, we get

$$\mu_{2,D} = \mu_{2,d.v.} + \frac{2}{H k_L a_B}\left(\frac{V_L}{Q}\right) \qquad (26)$$

With the value of $k_La_B$ determined for the nitric oxide-water system (see Table 2), the second term in Equation (26) at $Q$ = 3.33 cm/s for the nitrogen-saturated sodium chloride solution ($H$ = 384) is 80 s². The bubbles for the nitrogen-sodium chloride-water system were observed to be much smaller than those for the nitric oxide-water, system. Then, $k_La_B$ for nitrogen-sodium chloride-water would be greater than for nitric oxide-water, and the magnitude of the second term in Equation (26) would be less than 80s². Since the measured value of $\mu_{2,D}$ was much greater, 1 500 s², little error is introduced by taking $\mu_{2,d.v.}$ equal to the second moment, that is, $\mu_{2,D}$ determined from breakthrough curves for the nitrogen saturated sodium chloride solution. These values are also given in Table 2 and were used with Equation (18) to obtain $\mu_{2,L_1}$ for the nitric oxide-slurry system. As an illustration of magnitudes of the moments, at $Q$ = 3.33 cm³/s for $R$ = 0.0015 cm, $\mu_{2,D}$ was about 13 000 s² for the slurry, 3 300 s² for the nitric oxide-water system, and $\mu_{2,d.v.}$ = 1 500 s².

## MASS TRANSFER FROM BUBBLE TO LIQUID

For determination of the rate coefficients, it is helpful to rearrange Equation (15) to the form

$$\mu_{2,L_1}\left(\frac{Q}{V_L}\right)=\frac{2}{H}\left[\left(\frac{R}{5D_e a_s}+\frac{1}{k_s a_s}\right)\left(m_s\frac{\beta}{\rho_p}+m_s K\right)^2+\frac{m_s K^2}{k_{ads}}\right]+\left(\frac{m_s K+1}{H}\right)^2\frac{1+e^{-\alpha L}}{1-e^{-\alpha L}}\left(\frac{V_L}{Q}\right) \quad (27)$$

The quantity $\alpha L$ is independent of $Q$ since both $a_B$ and $V_B$ in Equation (16) are proportional to $Q$ [Equations (22) and (23)]. Hence, a plot of $\mu_{2,L_1}$ $(Q/V_L)$ vs. $V_L/Q$ should be a straight line with a slope dependent upon $k_L$ [through $\alpha$, Equation (16)] and an intercept which is a function of the other rate coefficients $k_s$, $D_e$, and $k_{ads}$. For the conditions of our experiments, the data show that the terms in Equation (27) involving $k_L$, $D_e$, and $k_{ads}$ are all important. Hence, the contributions to $\mu_{2,L_1}$ for $k_L$ and $D_e$ must be separated before $k_{ads}$ can be determined.

Figure 7 illustrates the data plotted according to Equation (27) for each particle size. The slopes for $R$ = 0.0015 and 0.083 cm are nearly the same, indicating that $k_L$ was not affected by the size of carbon particles. From the values given in Table 2 for slurry conditions, and by using Equations (16) and (21), $k_L$ = 0.27 cm/s.

The bubble-to-liquid coefficient can also be obtained from breakthrough curve data for nitric oxide and water alone. For this situation, Equation (27) reduces to

$$\mu_{2,L_1}=\left(\frac{1}{H^2}\right)\frac{1+e^{-\alpha L}}{1-e^{-\alpha L}}\left(\frac{V_L}{Q}\right)^2 \quad (28)$$

Figure 8, displaying the data plotted as $\mu_{2,L_1}$ vs. $(V_L/Q)^2$, does give a zero intercept as indicated by Equation (28). Then the difference in intercepts in Figures 7 and 8 shows that $k_s$, $D_e$, and $k_{ads}$ either individually or in combination significantly affect the overall adsorption process. The slope of the line in Figure 8 corresponds to $k_L$ = 0.25 cm/s. Since this result is not significantly different from $k_L$ determined from Figure 7, it is concluded that carbon particles did not have a measurable effect on the bubble-to-liquid mass transfer coefficient.

Because of potential error in $a_B$ for the bubbles, there is considerable uncertainty in these results for $k_L$. Equation (1) does not include a term for the mass transfer at the liquid-gas interface at the top of the slurry. Owing to the small number of bubbles, this interfacial area is not negligible with respect to $a_B$. Omission of the term gives erroneously high values for $k_L$ for the bubbles. It was observed that the bubble velocity was higher in the region near the impeller. This could also result in mistakenly high values for $k_L$. Finally, extreme turbulence caused by the impeller could result in bubble areas $a_B$ higher than predicted by Equation (22), because the vertical velocity component in a slurry with agitation could be different from that determined as 22.5 cm/s in an unagitated vessel. Misic and Smith (1971) found $k_L$ to be about 0.04 cm/s for benzene dissolving in water in a more mildly agitated, small diameter (4.0 cm) vessel for which the gas-liquid interfacial area at the top of the slurry was much less than for our adsorber (10 cm diameter). The correlation of Prasher and Wills (1973) gives $k_L$ = 0.10 cm/s at the energy dissipation rate [4.4 × $10^4$ erg/(s)(g liq)] of the impeller in our

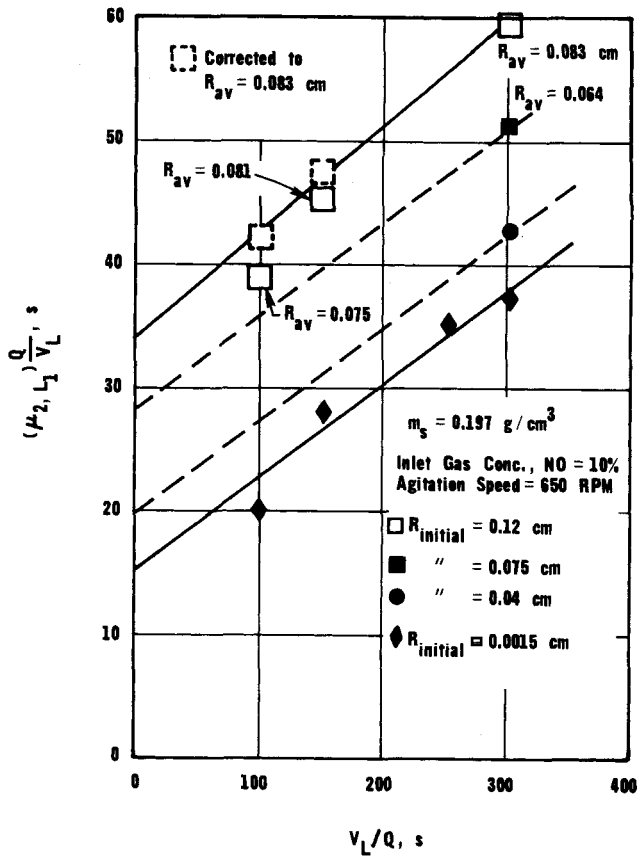


Fig. 7. Second moment data for the nitric oxide-water-carbon system.

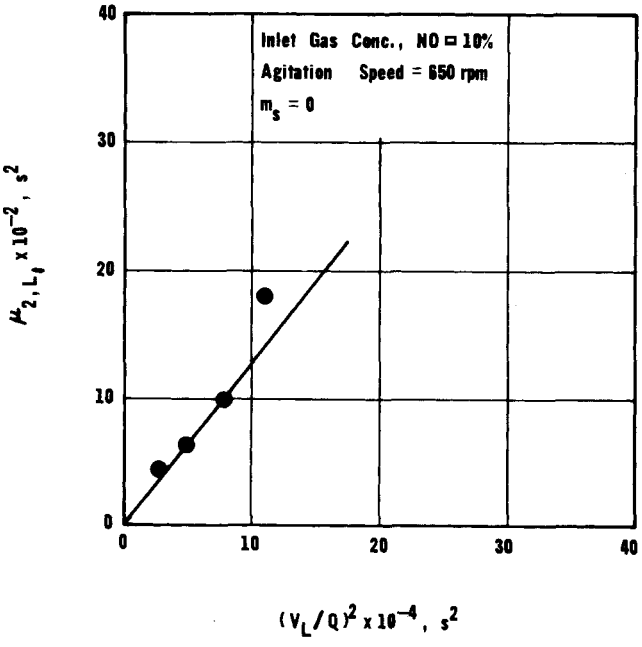


Fig. 8. Second moment data for the nitric oxide-water system.

system. This dissipation rate was known for the geometry and impeller rotation speed of our system from the work of Furusawa and Smith (1973*a*). Calderbank (1967) in a summary of $k_L$ for various systems found most values to be less than 0.1 cm/s, which is considerably less than 0.27 cm/s.

The uncertainty in $k_L$ alone does not affect subsequent analysis of the data for $k_s$, $D_e$, and $k_{ads}$. As Equation (27) shows, the intercept depends only on the product $k_L a_B$. Much of the uncertainty in all $k_L$ values is due to inaccuracy in the area term $a_B$.

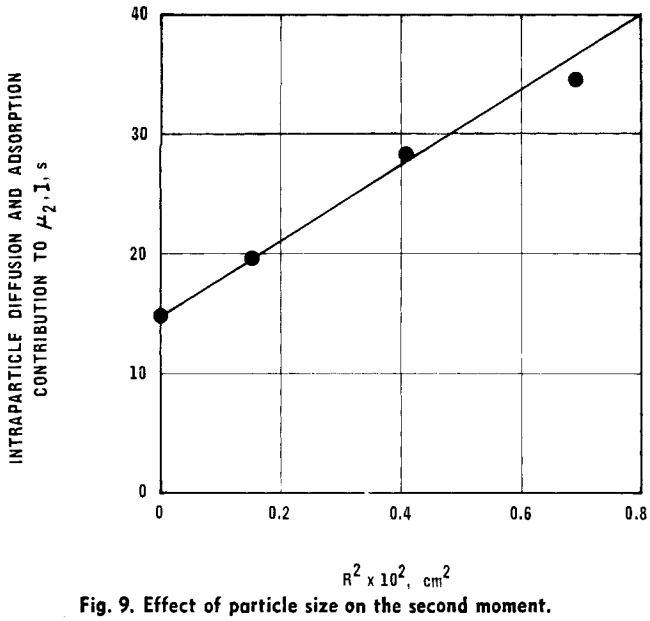


**Fig. 9. Effect of particle size on the second moment.**

## MASS TRANSFER FROM LIQUID TO PARTICLE

In order to evaluate $k_{ads}$ and $D_e$ as accurately as possible, the contributions of $k_s a_s$ to the intercepts in Figure 7 were minimized. This was accomplished by increasing $a_s$. For the conditions employed, $a_s$ ranged from 493 cm$^{-1}$ for the smallest particles to 8.9 cm$^{-1}$ for the largest particles. From the data and correlations given by Furusawa and Smith (1973*a*), the corresponding range of $k_s$ is approximately 0.030 to 0.018 cm/s. Then, for the largest particles, where the effect of $k_s a_s$ would be greatest, $k_s a_s$ is about 0.16 s$^{-1}$. For this situation, the term involving $1/k_s a_s$ is but 2.5% of the total intercept in Figure 7 and may be neglected.

## INTRAPARTICLE DIFFUSIVITY AND ADSORPTION RATE CONSTANT

From Equation (27), with $1/k_s a_s$ neglected, the intercepts in Figure 7 are given by

$$I = \frac{2m_s}{H}\left[\frac{Rm_s}{5D_e a_s}\left(\frac{\beta}{\rho_p} + K\right)^2 + \frac{K^2}{k_{ads}}\right] \quad (29)$$

Since $a_s = 3m_s/\rho_p R$ for spherical particles, Equation (29) may be written

$$I = \frac{2m_s}{H}\left[\frac{R^2\rho_p}{15D_e}\left(\frac{\beta}{\rho_p} + K\right)^2 + \frac{K^2}{k_{ads}}\right] \quad (30)$$

This result shows that the intercept $I$ should be a linear function of $R^2$ and that the slope of the line establishes $D_e$ and the intercept $k_{ads}$. The intercepts shown in Figure 7 are plotted vs. $R^2$ in Figure 9.

Before we examine Figure 9, the intercepts for the largest particle size initial $R = 0.12$ in Figure 7 need to be explained. For large particle sizes, the agitation in the slurry caused considerable attrition. Examination showed that the particles did not break into two or more parts but that corners and edges, where the radius of curvature was small, suffered attrition. In order to minimize such attrition during a run, the fresh particles were first pretreated in a water slurry under mild agitation conditions. These pretreated particles, after drying and sieving, were employed for the adsorption runs and had the radii designated as initial values in Table 1 and Figure 9. After this pretreatment, some additional attrition occurred. Hence, average particle radii were determined from size measurements before and after a run. The radii shown beside the open squares in Figure 7 represent such average values for the two largest particles. Since such average radii were somewhat different for the runs at different flow rates made for the largest particles, the values of $(\mu_{2,L_1})Q/V_L$ were corrected to the same $R$ of 0.083 cm. This correction was made by taking the intraparticle diffusion contribution to be proportional to the square of the radius, as suggested by Equation (30). The open, dotted squares in Figure 9 represent such corrected points. The line through the corrected points for $R = 0.083$ cm was used to obtain the intercept for the largest particle size. Measurable attrition did not occur for the two smallest particles. The radius of the second largest size was reduced from an initial value of 0.075 to 0.064 cm by attrition during the run.

From the intercept and slope of the straight line in Figure 9, as defined by Equation (30), $k_{ads}$ and $D_e$ were calculated to be $5.8 \times 10^{-2}$ cm./(g)(s) and $1.8 \times 10^{-5}$ cm/s, respectively. To our knowledge this is the first time that rates of adsorption for nitric oxide from aqueous solution on carbon have been determined. The rate coefficient is rather low, suggesting chemisorption. Solbakken and Reyerson (1960) have proposed that nitric oxide adsorption on alumina gel involves electron spin multiplicity changes. Such processes have small transmission coefficients and low rates. Perhaps this kind of phenomenon occurs on activated carbon, which also has excess electrons. The rate constant for oxygen adsorption on the same carbon was 2.2 cm$^3$/(g)(s) (Komiyama and Smith, 1975).

The effective diffusivity is of the expected magnitude. Since no experimental data were available for the molecular diffusivity of nitric oxide in water, an accurate value of the tortuosity factor cannot be obtained. An approximate value can be estimated by using correlations for predicting the molecular diffusivity at infinite dilution at 25°C. Wilke and Chang's correlation gives $2.55 \times 10^{-5}$ cm$^2$/s. Sheibel's gives $2.67 \times 10^{-5}$ cm$^2$/s, and Thaker's equation gives $2.39 \times 10^{-5}$ cm$^2$/s (Reid and Sherwood, 1966). By taking an average value of $2.54 \times 10^{-5}$, and with the porosity of 0.60, the tortuosity factor $\gamma$ is

$$\gamma = \frac{\beta D_{NO-H_2O}}{D_e} \sim 0.9 \quad (31)$$

Tortuosity factors in liquid-filled pores are not well established. From adsorption studies of physically adsorbed substances such as benzaldehyde on activated carbon and on Amberlite particles, tortuosity factors as low as 0.3 have been reported (Furusawa and Smith, 1973*a*; Komiyama and Smith, 1974). Tortuosity factors calculated from reaction data have usually been of the order of those for gas-filled pores, that is 1 to 5 (Kenney and Sedriks, 1972; Komiyama and Smith, 1975). Since surface diffusion is not expected to be significant for our system, where the rate and extent of adsorption are low, this phenomenon is unlikely to explain the low tortuosity factor. It is possible that the calculated molecular diffusivity of nitric oxide in water is not applicable in the small pores of activated carbon (average radius = 13Å) because of interaction between the polar nitric oxide molecules adsorbed and in the liquid. Since both nitric oxide and carbon are paramagnetic, diffusion in the micropores could be influenced by magnetic effects. These explanations are speculative, and more study is needed on effective diffusivities in liquid-filled pores, particularly in systems where surface diffusion is insignificant.

## MIXING OF GAS BUBBLES IN SLURRIES

As mentioned earlier, the mixing state of the gas bubbles is somewhat uncertain. The equations for $\mu_2$ presented up to this point have been based upon vertical, plug flow through the slurry. For a highly agitated slurry, it is conceivable that the bubbles could approach a state of complete mixing, complete mixing in the sense that the concentration of adsorbate would be the same in all bubbles of the slurry and not in the sense that the bubbles would coalesce and mix. It would be helpful to have a test for the extent to which the mixing state affects the observed second moment, since this influences the analysis for other rate constants $k_{ads}$, $D_e$, $k_s$. Such a test can be developed by comparing second-moment expressions for plug flow and complete mixing.

Since the contributions of the several transport processes to the second moment are additive and independent [for example, Equation (15)], it is satisfactory to make the comparison for the case where bubble-to-liquid mass transfer is rate determining. Then, for plug flow, Equation (15) reduces to

$$(\mu_{2,L_1})_{PF} = \left(\frac{m_sK+1}{H}\right)^2 \frac{1+e^{-\alpha L}}{1-e^{-\alpha L}} \left(\frac{V_L}{Q}\right)^2 \tag{32}$$

For complete mixing, mass balances for the gas and liquid phases become, for $t > 0$

$$\frac{Q}{V_L} C_g + k_L a_B \left(\frac{C_g}{H} - C_L\right) = -V_B \frac{\partial C_g}{\partial t} \tag{33}$$

$$k_L a_B \left(\frac{C_g}{H} - C_L\right) = (m_sK+1) \frac{\partial C_L}{\partial t} \tag{34}$$

Solution for a pulse input [Equation (5)], following the procedure used to solve Equations (1) to (8), gives the following expressions for the moments:

$$(\mu_{1,L_1})_{ST} = \left(V_B + \frac{m_sK+L}{H}\right)\frac{V_L}{Q} = \frac{m_sK+1}{H}\left(\frac{V_L}{Q}\right) \tag{35}$$

$$(\mu_{2,L_1})_{ST} = \frac{2}{k_L a_B}\frac{(m_sK+1)^2}{H}\left(\frac{V_L}{Q}\right) + \left(V_B + \frac{m_sK+1}{H}\right)^2\left(\frac{V_L}{Q}\right)^2$$

$$= \frac{2}{k_L a_B}\frac{(m_sK+1)^2}{H}\left(\frac{V_L}{Q}\right) + \left(\frac{m_sK+1}{H}\right)^2\left(\frac{V_L}{Q}\right)^2 \tag{36}$$

The second equalities in Equations (35) and (36) arise because for the conditions of our work, $V_B$ was much less ($10^{-3}$ vs. $10^{-1}$) than $(m_sK+1)/H$.

For very large $k_L a_B$ (large $\alpha L$), Equations (32) and (36) reduce to the same value for $\mu_{2,L_1}$:

$$(\mu_{2,L_1})_{PF} = (\mu_{2,L_1})_{ST} = \left(\frac{m_sK+1}{H}\right)^2\left(\frac{V_L}{Q}\right)^2 \tag{37}$$

For very small $k_L a_B$ (small $\alpha L$), the exponential functions can be expanded in power series, and higher terms neglected, to give

$$\frac{1-e^{-\alpha L}}{1-e^{-\alpha L}} = \frac{2}{\alpha L} = \frac{2H}{k_L a_B}\left(\frac{Q}{V_L}\right)$$

Then, Equations (32) and (36) again become identical:

$$(\mu_{2,L_1})_{PF} = (\mu_{2,L_1})_{ST} = \frac{2}{k_L a_B}\frac{(m_sK+1)^2}{H}\left(\frac{V_L}{Q}\right) \tag{38}$$

The identical values of $\mu_2$ and, hence $k_L a_B$, for complete mixing and plug flow for either extreme of mass transfer rate is physically understandable. For large transfer rates, large $k_L a_B$, equilibrium between concentrations in the bubble and in the liquid is established very quickly after the bubble leaves the disperser. Then the concentration in the gas bubble is essentially constant throughout the slurry, and the mixing state of the bubbles is immaterial. This was the situation found by Komiyama and Smith (1975) for the adsorption of sulfur dioxide, which is relatively soluble in water. For small values of $k_L a_B$, little mass is transferred from the bubbles in their path through the slurry. Again, the concentration in the bubbles is nearly constant throughout the slurry.

To test for the effect of the mixing state on $\mu_2$, values of $k_L a_B$ should be determined from the data by using equations for complete mixing and for plug flow. If the two values are nearly the same, the mixing state has little effect on the results. If the two values are widely different, the mixing state has an effect. Then, an accurate evaluation of $k_L a_B$ requires more information about the flow pattern of the gas bubbles. To illustrate, with the data shown for the nitric oxide-water system in Figure 8, $k_L a_B$, determined from the plug flow equation at a flow rate of 3.33 cm³/s was 0.020 $s^{-1}$, while that determined for complete mixing, Equation (36) with $m_s = 0$, was 0.023 $s^{-1}$. The difference is within the range of experimental error, so it is concluded that the mixing state did not affect the value of $k_L a_B$.

These conclusions do not apply to values of $k_L$ themselves but to the product $k_L a_B$. Fortunately, only the product is needed in order to continue with the analysis and evaluate $k_s a_s$, $D_e$, and $k_{ads}$. Separate values of $k_L$ are subject to large uncertainties because of the lack of accurate knowledge of $a_B$.


## ACKNOWLEDGMENT

The financial support of the National Science Foundation through Grant GK-38881 is gratefully acknowledged. Also, we thank the Calgon Corporation, Pittsburgh Activated Carbon Division, for providing samples of activated carbon.


## NOTATION

$a_B$ = surface area of bubbles per unit volume of bubble and solid-free liquid, $cm^{-1}$
$a_s$ = outer surface area of particles per unit volume of bubble and solid-free liquid, $cm^{-1}$
$C_g$ = concentration of adsorbate in gas (bubble) phase, mole/cm³
$\tilde{C}_g$ = Laplace transform of $C_g$
$C_i$ = concentration of adsorbate in pore space, mole/cm³
$C_L$ = concentration of adsorbate in bulk liquid, mole/cm³
$D_{NO\text{-}H_2O}$ = molecular diffusivity of nitric oxide in water at infinite dilution, cm²/s
$D_e$ = effective intraparticle diffusivity, cm²/s
$H$ = Henry's constant for adsorbate in water, $H = C_g/C_L$
$I$ = contribution of intraparticle diffusion and adsorption to second moment, s²
$k_{ads}$ = adsorption rate constant, cm³/(g)s
$k_L$ = bubble-to-liquid mass transfer coefficient, cm/s
$k_s$ = liquid-to-particle mass transfer coefficient, cm/s

$K$ = adsorption equilibrium constant, $cm^3/g$
$L_1$ = height of slurry, cm; region $L_1$ to $L_2$ is gas collecting space above slurry
$m_n$ = moment component, defined by Equation (10)
$m_s$ = mass of carbon per unit volume of bubble and solid free liquid, $g/cm^3$
$n$ = amount of adsorbed nitric oxide, mole/g
$Q$ = gas feed rate at 25°C and 1 atm, $cm^3/s$
$r$ = radial coordinate in a spherical particle, measured from its center, cm
$R_B$ = average radius of gas bubbles, cm
$R$ = radius of spherical particle, cm
$s$ = Laplace variable
$S_{BET}$ = BET surface area, $m^2/g$
$t$ = time, s
$v_B$ = vertical bubble velocity, cm/s
$V_B$ = bubble volume per unit volume of bubble and solid-free liquid
$V_L$ = total volume of liquid in the vessel, $cm^3$
$z$ = slurry height, measured from bottom of the vessel, cm

**Greek Letters**

$\alpha$ = bubble-to-liquid rate parameter defined by Equation (16), $cm^{-1}$
$\beta$ = particle porosity
$\delta(0)$ = input pulse, Dirac delta function with an infinite value at $t = 0$
$\mu'_{1,L_1}$ = first absolute moment in the slurry, or for the liquid when no particles are present, s
$\mu'_{1,d.v.}$ = first absolute moment in the dead volumes, s
$\mu'_{1,D}$ = first absolute moment evaluated at the detector, s
$\mu_{2,L_1}$ = second central moment for the slurry; $\mu_{2,d.v.}$ and $\mu_{2,D}$ are second moments for the dead volumes and as measured at the detector, respectively, $s^2$
$\rho_p$ = particle density, $g/cm^3$
$\rho_t$ = solid-phase density, $g/cm^3$
$\gamma$ = tortuosity factor

**Subscripts**

$L_1, L_2$ = value at $z = L_1$ and $L_2$ respectively
$b, \delta$ = responses to step and pulse ($\delta$) inputs
$o$ = inlet value
$PF$ = gas bubbles in plug flow through slurry
$ST$ = gas bubbles completely mixed in slurry

**LITERATURE CITED**


Calderbank, P. H., "Mixing," V. W. Uhl and J. B. Gray, ed., Vol. II, p. 65, Academic Press, New York (1967).

Furusawa, T., and J. M. Smith, "Fluid-Particle and Intraparticle Mass Transfer Rate in Slurries," *Ind. Eng. Chem. Fundamentals*, **12**, 197 (1973*a*).

———, "Mass Transfer Rate in Slurries by Chromatography," *ibid*, 360 (1973*b*).

Furusawa, T., and M. Suzuki, "Moment Analysis of Concentration Decay in a Batch Adsorption Vessel," *J. Chem. Eng. Japan*, **8**, 119 (1975).

Kenney, C. N., and W. Sedriks, "Effectiveness Factors in a Three-Phase Slurry Reactor," *Chem. Eng. Sci.*, **27**, 2029 (1972).

Juvekar, V. A., and M. M. Sharma, "Adsorption of $CO_2$ in a Suspension of Lime," *ibid.*, **28**, 825 (1973).

Komiyama, H., and J. M. Smith, "Sulfur Dioxide Oxidation in Slurries of Activated Carbon. Part I. Kinetics," *AIChE J.*, **21**, 664 (1975); "Part II. Mass Transfer Studies," *ibid.*, 670.

———, "Surface Diffusion in Liquid-Filled Pores," *ibid.*, **20**, 1110 (1974).

Linke, W. F., "Solubilities," American Chemical Society, Washington, D.C. (1965).

Misic, D. M., and J. M. Smith, "Adsorption of Benzene in Carbon Slurries," *Ind. Eng. Chem. Fundamentals*, **10**, 380 (1971).

Prasher, B. D., and G. B. Wills, "Mass Transfer in an Agitated Vessel," *Ind. Eng. Chem. Process Design Develop.*, **12**, 351 (1973).

Reid, R. G., and T. K. Sherwood, "The Properties of Gases and Liquid," 2 ed., McGraw-Hill, New York (1966).

Satterfield, C. N., "Mass Transfer in Heterogeneous Catalysis," pp. 38-39, 119-120, M.I.T. Press, Cambridge, Mass. (1970).

Sherwood, T. K., and E. J. Farkas, "Studies on the Slurry Reactor," *Chem. Eng. Sci.*, **21**, 573 (1966).

Siems, W., and W. Weiss, "Mixing of Liquid by Means of Gas Bubbles in Narrow Columns," *Chem. Eng. Tech.*, **29**, 727 (1957).

Solbakken, A., and L. H. Reyerson, "Sorption and Magnetic Susceptibility Studies on Nitric Oxide—Alumina Gel Systems at Several Temperatures," *J. Phys. Chem.*, **64**, 1903 (1960).

Valentin, F. H. H., "Absorption in Gas-Liquid Dispersions," E. and F. N. Spon, Ltd., London, England (1967).



*Manuscript received February 19, 1976; revision received April 16, and accepted April 20, 1976.*


# Separation Sequence Synthesis by a Predictor Based Ordered Search


**ALEJANDRO GOMEZ M.**

**and**

**J. D. SEADER**

**Department of Chemical Engineering**
**The University of Utah**
**Salt Lake City, Utah 84112**



A predictor based ordered search procedure is used to scan the graph representing all possible separation sequences for a given multicomponent separation process. The algorithmic procedure is expedited by utilizing an heuristic cost function to obtain lower bound estimates of the cost of separators not yet designed. Considerable reduction in search space occurs. Optimal and near optimal sequences are readily generated.


## SCOPE

Many chemical processes involve separation sequences, wherein multicomponent feed mixtures are separated into products (including recycle or intermediate streams) by two or more separators. As shown by Thompson and King (1972*a*), the number of possible processing schemes or sequences (arrangements of separators) increases exponentially with the number of products and with the number of different types of separators being considered.


Correspondence concerning this paper should be addressed to J. D. Seader.